Fast Computation of Accurate Pseudo Zernike Moments for Binary and Gray-Level Images

Khalid Hosny
Faculty of Computers and Informatics, Zagazig University, Egypt

Abstract: *A new method is proposed for fast computation of accurate pseudo-Zernike moments for binary and gray level images. These orthogonal moments are computed as a linear combination of accurate geometric and radial geometric moments, which are computed by mathematical integration of the monomial polynomials over digital image pixels. The proposed method is fast, accurate, simple, and easy programmable. A comparison with the existing methods is performed. The obtained results explain the efficiency of the proposed method.*

Keywords: *Pseudo-Zernike moment, geometric moments, symmetry property, fast computation, binary images, gray level images.*

Received September 20, 2011; accepted May 22, 2012; published online April 4, 2013

1. Introduction

Pseudo Zernike Moments (PZMs) are orthogonal moments defined by mapping an image onto a set of pseudo Zernike polynomials [5]. These polynomials are orthogonal complex polynomials defined in polar coordinates over a unit circle. Teague [22] introduced orthogonal moments as alternatives to the non-orthogonal moments in order to overcome their limited capabilities in image representation. The orthogonal moments are used to represent an image with the minimum amount of information redundancy [23]. In addition to this attractive property, ZMs and PZMs are rotation and flipping invariants by nature.

By experiment, Teh and Chin [23] showed that PZMs are superior to conventional ZMs in terms of their feature representation capabilities, and more robust to image noise. Mukundan and Ramakrishnan [19] in their famous book on moment functions compared PZMs with ZMs shows that, the first set of moments has more feature vectors for the same maximum order. For example, with a moment order equal to 10, the feature vector of PZMs has 66 dimensions while the corresponding one for ZMs has 36 dimensions. This property ensures the robustness of PZMs in the presence of image quantization error.

ZMs and PZMs are used in biometrics such as fingerprint and human face recognition [1, 8, 9, 13, 15, 16, 20, 21], and watermarking of digital images [14, 17, 24, 25], image registration [26], geometric object recognition [4] and Arabic handwriting recognition [6].

Despite of their better characteristics, the highly computational demands of the circular orthogonal PZMs hindered the wide application as in the case of ZMs. The direct computations through their polynomials are very time consuming procedures. Therefore, it is impractical to apply a direct method in any real world application. In addition to this, the computational process encounters more additional problems. These problems are related to the square to circle mapping transformation, where digital images are usually defined in the Cartesian coordinates while pseudo Zernike polynomials are by nature defined in the polar coordinates. Such transformation produced two kinds of errors. First, the geometric error is a result of the mapping transformation. Second; the numerical error is a result of approximation process.

To accelerate the computational procedures, two remarkable algorithms are proposed [2, 7]. The implemented methodology in these two works is very similar where the authors concentrate on reducing the computational processes through applying a kind of recursive relations to compute the real-valued radial functions. These algorithms marginally reduce the computational times and unfortunately produce sets of inaccurate moments, where the integrals are replaced by summations. In fact, the recursive computation approach saves execution times while the memory requirements are still problematic. This is very clear for big size images where the memory requirements of the Chong's method [7] are very high.

In [2], the author proposed a method to compute the real-valued radial pseudo Zernike functions, $\{S\}$, from the corresponding real-valued radial Zernike functions, $\{\Re\}$, by using the following relation:

$$S_{n,m}(r) = \Re_{2n+1,2m+1}\left(\sqrt{r}\right)\Big/\sqrt{r} \quad (1)$$

He implemented different well known methods to compute real-valued radial Zernike functions $\{\Re\}$. Unfortunately, in order to compute radial pseudo Zernike functions for the maximum order, *Max*, by

using equation 1, radial Zenike functions of order *(2Max+1)* are required. The implementation of this method monotonically increased the required memory. By converting to the Cartesian coordinates, the radial Zernike functions, $\{\Re\}$, will be defined at each image pixel, (x_i, y_j). Therefore, these functions, $\Re_{p,q}(x_i, y_j)$, will be represented by four-dimensional array. The first index p is defined from "0" to "*Max*". The second index q is defined from "0" to "p" according to the condition, *(p-q)=even*. The third and fourth indices are defined from "0" to "*N-1*," where $N \times N$ is the size of the input image. Based on this explanation, increasing the maximum order from *Max* to (*2Max+1*), requires a huge memory and time-consuming computational process.

This paper proposes a very fast method for accurate computation of PZMs. This method consists of three steps. In the first step, the input image is mapped inside the unit circle with a modified mapping transformation, where a kind of symmetry property is applied to reduce the computational complexity. Then, accurate geometric and radial geometric moments are computed by using mathematical integration of monomials over the mapped image pixels. Finally, accurate PZMs are computed as a linear combination of geometric and radial geometric moments. The proposed method completely removes the time-consuming process of computing radial pseudo Zernike functions. The conducted numerical experiments clearly show the efficiency of the proposed method.

The rest of the paper is organized as follows: In section 2, a concise description of PZMs is presented, followed by the description of the proposed method in section 3. Numerical experiments are discussed in section 4. The conclusion is presented in section 5.

2. Pseudo Zernike Moments

The complex PZMs of order p and repetition q are defined as [19]:

$$A_{p,q} = \frac{p+1}{\pi} \int_0^{2\pi} \int_0^1 \overline{W_{p,q}(r,\theta)} f(r,\theta)\, r\, dr\, d\theta \qquad (2)$$

Where $p = 0, 1, 2, 3, \ldots, \infty$ and q is non-negative integer defined according to the condition $q \le p$. PZMs with negative values of q are computed from those of non-negative values by using the relation, $A_{p,-q} = \overline{A_{p,q}}$. Pseudo Zernike polynomials, $W_{pq}(r,\theta)$, are complex functions defined over a unit disk by multiplying the real valued-radial functions, $S_{p,q}(r)$, and the circular function, $e^{\hat{\imath} q \theta}$ as follows:

$$W_{p,q}(r,\theta) = S_{p,q}(r)\, e^{\hat{\imath} q \theta} \qquad (3)$$

These polynomials are orthogonal where their orthognality relation is written as:

$$\int_0^{2\pi} \int_0^1 W_{n,m}(r,\theta) \overline{W_{p,q}(r,\theta)}\, r\, dr\, d\theta = \begin{cases} \frac{\pi}{(p+1)}, & p = n, q = m \\ 0, & otherwise \end{cases} \qquad (4)$$

The real-valued radial functions, $S_{p,q}(r)$, could be explicitly expressed as a linear function of the variable, r, as follows:

$$S_{p,q}(r) = \sum_{k=q}^{p} B_{p,q,k}\, r^k \qquad (5)$$

With the coefficients:

$$B_{p,q,k} = \frac{(-1)^{(p-k)}(p+k+1)!}{(p-k)!(q+k+1)!(k-q)!} \qquad (6)$$

The direct computation of the coefficients, $B_{p,q,k}$, required calculation of four factorial terms plus the evaluation of an exponential function for every order p. This computational process is time and memory-consuming. To avoid these consuming processes, recurrence relations are derived where the coefficients, $B_{p,q,k}$, could be computed by using the following recurrence relations:

$$B_{p,p,p} = 1 \qquad (7)$$

$$B_{p,(q-1),p} = \frac{k+q+1}{k-q+1} B_{p,q,p} \qquad (8)$$

$$B_{p,q,(k-1)} = -\frac{(k+q+1)(k-q)}{(p+k+1)(p-k+1)} B_{p,q,k} \qquad (9)$$

The coefficients, $B_{p,q,k}$, are image-independent. Their dimensions are dependent only on the moment order. Therefore, these coefficients could be pre-computed and stored for future use.

Conventional computation of orthogonal PZMs is generally based on replacing integrals in equation 2 by summations, where the approximate PZMs are:

$$\tilde{A}_{pq} = \frac{p+1}{\lambda_p} \sum_{x=0}^{N-1} \sum_{y=0}^{N-1} S_{pq}(r_{ij})\, e^{-\hat{\imath} q \theta_{ij}} f(x,y) \qquad (10)$$

With $r_{xy} = \sqrt{x^2 + y^2}$ and $\theta_{xy}=arctan(y/x)$. The number λ_p refers to is the total number of pixels that achieves the condition $|r_{ij}| \le 1$. The reconstruction from orthogonal moments only adds the individual components of each order to generate the reconstructed image. Pseudo Zernike polynomials are used to decompose the image intensity function, $f(r,\theta)$, as follows:

$$f(r,\theta) = \sum_{p=0}^{\infty} \sum_{q} A_{p,q} W_{p,q}(r,\theta) \qquad (11)$$

The coefficients, $A_{p,q}$, are the PZMs of order p and repetition q. Since the summation to infinity is impossible in computing community, Zernike moments of maximum order equal to *Max* be considered where

the image intensity function is approximated as follows:

$$\hat{f}_{Max}(r,\theta) \approx \sum_{p=0}^{Max} \sum_{q} A_{p,q} W_{p,q}(r,\theta) \qquad (12)$$

3. The Proposed Method

The proposed method is a numerical precipice for fast and accurate computation of PZMs. A proper image mapping is employed in order to minimize the effect of geometric error. Then, a symmetry property is applied in order to reduce the computational complexity by 75%. Accurate PZMs are computed as a linear combination of accurate geometric and radial geometric moments, where these moments are accurately computed by using mathematical integration of monomials over image pixels. A fast algorithm is employed to significantly reduce the computational complexity.

The input digital image of size $N \times N$ as depicted in Figure 1-a is mapped inside the unit circle by using the mapping transformations:

$$x_i = \frac{2i-N-1}{N\sqrt{2}}, \; y_j = \frac{2j-N-1}{N\sqrt{2}} \qquad (13)$$

With $i, j = 1, 2, ..., N$ and the sampling intervals, Δx_i and Δy_j, have a constant value equal to $\sqrt{2}/N$. Each pixel of the mapped image is represented by one point in its centre, where the image intensity function is defined only for this discrete set of points $(x_i, y_j) \in [-1/\sqrt{2}, 1/\sqrt{2}] \times [-1/\sqrt{2}, 1/\sqrt{2}]$, as shown in Figure 1-b.

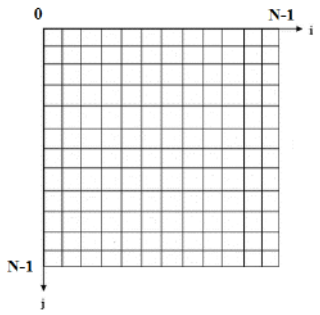

a) Image plane.

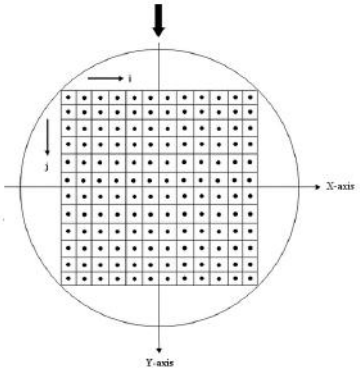

b) Square- to-circle mapping of the image plane.

Figure 1. Image mapping.

3.1. Accurate Pseudo Zernike Moments

Orthogonal PZMs are expressed in terms of geometric and radial geometric moments [3] as follows:

$$A_{p,q} = \frac{p+1}{\pi} \left[\{A_1\}_{k-q=even} + \{A_2\}_{k-q=odd} \right] \qquad (14)$$

With

$$A_1 = \sum_{k=q}^{p} \sum_{j=0}^{S_1} \sum_{m=0}^{q} \left(-\hat{i}\right)^m C_j^{S_1} C_m^q \, B_{p,q,k} \, G_{k-2j-m,\,2j+m} \qquad (15)$$

$$A_2 = \sum_{k=q+1}^{p} \sum_{j=0}^{S_2} \sum_{m=0}^{q} \left(-\hat{i}\right)^m C_j^{S_2} C_m^q \, B_{p,q,k} \, H_{k-2j-m-1,\,2j+m} \qquad (16)$$

Where $S_1=(k-q)/2$, $S_2=(k-q-1)/2$ and $\hat{i} = \sqrt{-1}$. The geometric and radial geometric moments $G_{p,q}$ and $H_{p,q}$ are defined as follows:

$$G_{p,q} = \int_x \int_y x^p y^q f(x,y)\, dx\, dy \qquad (17)$$

$$H_{p,q} = \int_x \int_y x^p y^q h(x,y)\, dx\, dy \qquad (18)$$

With:

$$h(x,y) = \left(x^2 + y^2\right)^{\frac{1}{2}} f(x,y) \qquad (19)$$

Direct computation of orthogonal PZMs by using equation 14 is time-consuming. Similar to our successfully approach for fast computation of accurate Zernike moments [12], a fast method for accurate pseudo Zernike moments for binary and gray level images is proposed. Equation 14 is rewritten as follows:

$$A_{p,q} = \frac{p+1}{\pi} \times \left\{ \sum_{\substack{k=q \\ k-q=even}}^{p} B_{p,q,k} \, R^G{}_{k,q} + \sum_{\substack{k=q+1 \\ k-q=odd}}^{p} B_{p,q,k} \, R^H{}_{k,q} \right\} \qquad (20)$$

$$R^G{}_{k,q} = \sum_{j=0}^{S_1} \sum_{m=0}^{q} \left(-\hat{i}\right)^m C_j^{S_1} C_m^q \; G_{k-2j-m,\,2j+m} \qquad (21)$$

$$R^H{}_{k,q} = \sum_{j=0}^{S_2} \sum_{m=0}^{q} \left(-\hat{i}\right)^m C_j^{S_2} C_m^q \; H_{k-2j-m,\,2j+m} \qquad (22)$$

The time-consuming direct computations of combinational terms in equations 21 and 22 are avoided by using the recurrence relations [12].

3.2. Accurate Radial Geometric Moments

Based on the equations 20, 21 and 22, radial moments are expressed as a linear combination of geometric and radial geometric moments. Therefore, efficient computation of these geometric moments represents the cornerstone of the whole computational process. As seen in Figure 1-b, both axes divide the transformed image into four quadrants. Each point P_1, with the Cartesian coordinates (x_i,y_j) in the first quadrant which has three similar points in the other three quadrants.

These points are $P_2(x_{N-i+1}, y_j)$, $P_3(x_{N-i+1}, y_{N-j+1})$ and $P_4(x_i, y_{N-j+1})$. All of these four points have the same radial distance from the origin point [12]. Based on this symmetry property, two augmented functions are defined based on the values of p and q. The augmented functions are defined as follows:

- Case 1: p and q are both even:

$$f_K(x_i,y_j) = f_1(x_i,y_j) + f_2(x_{N-i+1},y_j) + f_3(x_{N-i+1},y_{N-j+1}) + f_4(x_i,y_{N-j+1}) \quad (23)$$

$$h_K(x_i,y_j) = h_1(x_i,y_j) + h_2(x_{N-i+1},y_j) + h_3(x_{N-i+1},y_{N-j+1}) + h_4(x_i,y_{N-j+1}) \quad (24)$$

- Case 2: p is even and q is odd:

$$f_K(x_i,y_j) = f_1(x_i,y_j) + f_2(x_{N-i+1},y_j) - f_3(x_{N-i+1},y_{N-j+1}) - f_4(x_i,y_{N-j+1}) \quad (25)$$

$$h_K(x_i,y_j) = h_1(x_i,y_j) + h_2(x_{N-i+1},y_j) - h_3(x_{N-i+1},y_{N-j+1}) - h_4(x_i,y_{N-j+1}) \quad (26)$$

- Case 3: p is odd and q is even:

$$f_K(x_i,y_j) = f_1(x_i,y_j) - f_2(x_{N-i+1},y_j) - f_3(x_{N-i+1},y_{N-j+1}) + f_4(x_i,y_{N-j+1}) \quad (27)$$

$$h_K(x_i,y_j) = h_1(x_i,y_j) - h_2(x_{N-i+1},y_j) - h_3(x_{N-i+1},y_{N-j+1}) + h_4(x_i,y_{N-j+1}) \quad (28)$$

- Case 4: p and q are both odd:

$$f_K(x_i,y_j) = f_1(x_i,y_j) - f_2(x_{N-i+1},y_j) + f_3(x_{N-i+1},y_{N-j+1}) - f_4(x_i,y_{N-j+1}) \quad (29)$$

$$h_K(x_i,y_j) = h_1(x_i,y_j) - h_2(x_{N-i+1},y_j) + h_3(x_{N-i+1},y_{N-j+1}) - h_4(x_i,y_{N-j+1}) \quad (30)$$

Where $f_1(x_i,y_j)$ and $h_1(x_i,y_j)$ are the intensity functions in the first quadrant; the functions $f_2(x_{N-i+1}, y_j)$, $h_2(x_{N-i+1}, y_j)$, $f_3(x_{N-i+1}, y_{N-j+1})$, $h_3(x_{N-i+1}, y_{N-j+1})$, $f_4(x_i, y_{N-j+1})$ and $h_4(x_i, y_{N-j+1})$ are the intensity functions at the corresponding pixel points in the second, third and fourth quadrants respectively.

Geometric and radial geometric moments, $G_{p,q}$ and $H_{p,q}$, of order $(p+q)$ are computed accurately by mixing the discussed symmetry property and a modified version of our method [10] as:

$$G_{p,q} = \sum_{i=1}^{\lfloor \frac{N}{2} \rfloor} \sum_{j=1}^{\lfloor \frac{N}{2} \rfloor} I_p(x_i)\, I_q(y_j) f_K(x_i,y_j) \quad (31)$$

$$H_{p,q} = \sum_{i=1}^{\lfloor \frac{N}{2} \rfloor} \sum_{j=1}^{\lfloor \frac{N}{2} \rfloor} I_p(x_i)\, I_q(y_j) h_K(x_i,y_j) \quad (32)$$

Where:

$$\left\lfloor \frac{N}{2} \right\rfloor = \begin{cases} (N-1)/2, & N \text{ is odd} \\ N/2, & N \text{ is even} \end{cases} \quad (33)$$

$$I_p(x_i) = \frac{1}{p+1}\left[U_{i+1}^{\,p+1} - U_i^{\,p+1}\right] \quad (34)$$

$$I_q(y_j) = \frac{1}{q+1}\left[U_j^{\,q+1} - U_{j+1}^{\,p+1}\right] \quad (35)$$

With:

$$U_{i+1} = \frac{2i-N}{N\sqrt{2}} \text{ , } U_i = \frac{2(i-1)-N}{N\sqrt{2}} \quad (36)$$

The kernels, $I_p(x_i)$ and $I_q(y_j)$, are image independent; so the same kernels are used to compute accurate geometric and radial geometric. These kernels are pre-computed, stored and recalled whenever needed.

The computational complexity of equations 31 and 32 could be greatly reduced through the successive computation of the 1D q-th order moments for each row. These equations will be rewritten in a separable form as follows:

$$G_{p,q} = \sum_{i=1}^{\lfloor \frac{N}{2} \rfloor} I_p(x_i)\, Y^f{}_{i,q} \quad (37)$$

$$H_{p,q} = \sum_{i=1}^{\lfloor \frac{N}{2} \rfloor} I_p(x_i)\, Y^h{}_{i,q} \quad (38)$$

Where:

$$Y^f{}_{i,q} = \sum_{j=1}^{\lfloor \frac{N}{2} \rfloor} I_q(y_j) f_K(x_i,y_j) \quad (39)$$

$$Y^h{}_{i,q} = \sum_{j=1}^{\lfloor \frac{N}{2} \rfloor} I_q(y_j) h_K(x_i,y_j) \quad (40)$$

3.3. Pseudo-Code

For easy programming, all detailed processes are summarized through the steps of the following pseudo-code, where 2D PZMs are computed for input image of size $N \times N$. A maximum moment order, *Max*, is considered in all the conducted experiments.

Step 1: For i =1 to N+1
Compute $U_i = \frac{2(i-1)-N}{N\sqrt{2}}$
Step 2: For i =1 to N
Compute $x_i = \frac{U_{i+1}+U_i}{2}$ *& h(x_i,y_j)*
Step 3: For p = 0 to Max & For i = 1 to N
Construct the Kernel matrix $I_p(x_i)$ using equations 34 and 35
Step 4: For p = 0 to Max
Compute the coefficients, B, of pseudo Zernike polynomials
Step 5: For i = 1 to ⌊N/2⌋ and j = 1 to ⌊N/2⌋
Compute the augmented functions, $f_K(x_i,x_j)$ and $h_K(x_i,x_j)$ using equations 23 and 24
Step 6: For p = 0 to Max & For i = 1 to ⌊N/2⌋
Compute $Y^f{}_{i,q}$ and $Y^h{}_{i,q}$ using equations 39 and 40
Step 7: For p = 0 to Max & For q = 0 to Max-p
Compute accurate geometric and radial geometric, G_{pq} and H_{pq}, using equations 37 and 38
Step 8: For p = 0 to Max and q = 0 to Max-p

Compute $Y^{G}_{p,q}$ *and* $R^{H}_{p,q}$ *using equation 21*
Step 9: For p = 0 to Max-1 & For q = p
Compute $A_{p,q}$ *using equation 20*

4. Numerical Experiments

Numerical experiments are conducted with different sets of image database. Based on the discussion in introduction, the method [2] is excluded from the comparison. The performance for the proposed method is evaluated and compared with Chong's method [7]. Several numerical experiments are performed where the set of PZMs is computed using the proposed method and the method of Chong and his co-workers. The average elapsed CPU times are computed for different images and moment orders, where all numerical experiments are performed with 1.8GHz Pentium IV PC with 512 MBYTE RAM. The code is designed by using Matlab7.

The Execution-Time Improvement Ratio (ETIR) [12] is used as a criterion to compare the different computation methods and defined as ETIR=(*1-Time1/Time2*)×*100* where *Time1* and *Time2* are the execution-time of the first and the second methods, ETIR=0 if both execution times are identical.

A set of binary images of size 256×256 as showed in Figure 2 is used in the first numerical experiment. This set contains sixteen binary shapes. These shapes are selected from the MPEG7_Shape_1_Part_B database [18]. The CPU elapsed times and the execution-time improvement ratio for selected moment orders are included in Table 1. Average elapsed times are plotted against the moment order in Figure 3. It is clear that, the proposed method tremendously reduced the execution time.

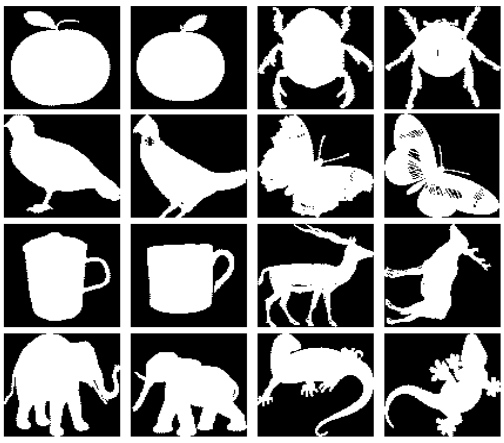

Figure 2. Binary images.

In the second and the third numerical experiments, a set of standard gray-level images as shown in Figure 4. The size 128×128 is used in the first experiment while the size 256×256 is used in the second experiment. The full set of PZMs is computed by using both methods. The CPU elapsed times and the execution-time improvement ratio are included in Tables 2 and 3. Elapsed times are plotted against the moment order in Figures 5 and 6. It is clear that, Chong's method is very time-consuming. On the other side, the proposed method is a very fast.

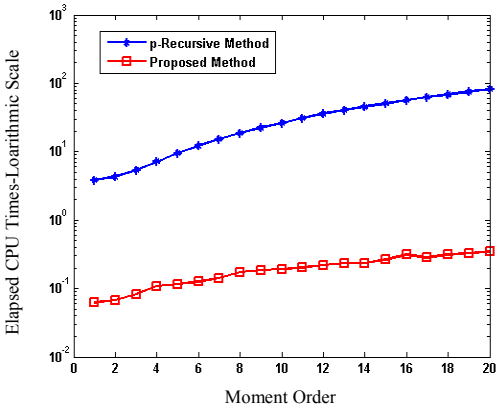

Figure 3. Graphical representation of average CPU times in seconds for the set of binary images of size 256×256.

Table 1. Average CPU times and percentage reduction for selected moment orders: Binary images of size 256×256.

Max	p-Recursive Method [7]	Proposed Method	Percentage of Reduction
1	3.8600	0.0620	98.39 %
5	9.5320	0.1150	98.79 %
10	26.3440	0.1920	99.27 %
15	50.6410	0.2660	99.47 %
20	81.9220	0.3440	99.58 %

Figure 4. A set of gray level images.

Table 2. Average CPU times and percentage reduction for selected moment orders: Gray level images of size 128×128.

Max	p-Recursive Method [7]	Proposed Method	Percentage of Reduction
1	0.8130	0.0110	98.64 %
5	2.1720	0.0280	98.71 %
10	5.1870	2.0470	99.09 %
15	9.3280	0.0790	99.15 %
20	16.2500	0.1080	99.33 %

Table 3. Average CPU times and percentage reduction for selected moment orders: Gray level images of size 256×256.

Max	p-Recursive Method [7]	Proposed Method	Percentage of Reduction
1	0.8130	0.0110	98.64 %
5	2.1720	0.0280	98.71 %
10	5.1870	2.0470	99.09 %
15	9.3280	0.0790	99.15 %
20	16.2500	0.1080	99.33 %

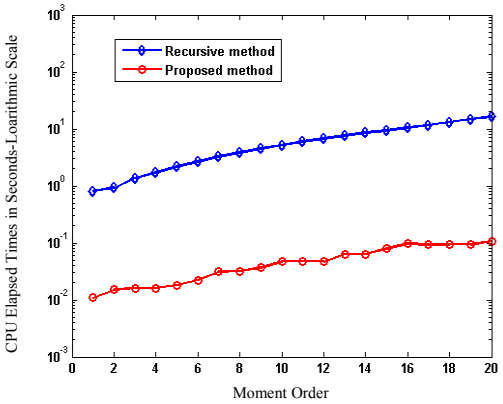

Figure 5. Graphical representation of average CPU times in seconds for the set of gray level images of size 128×128.

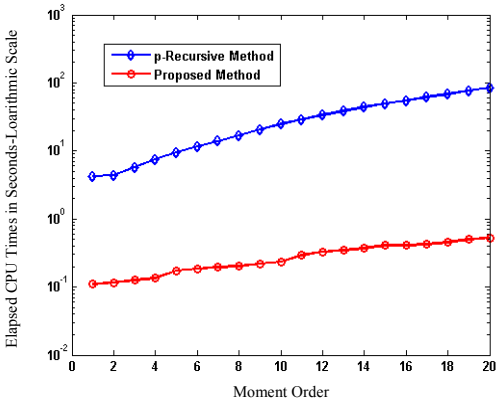

Figure 6. Graphical representation of average CPU times in seconds for the set of gray level images of size 256×256.

5. Conclusions

This paper proposes an algorithm for fast computation of 2D PZMs for binary and gray-level images. The proposed method completely removes the numerical errors where geometric and radial geometric moments are accurately computed through mathematical integrations over the image pixels. The proposed method saves 75% of the whole computational complexity by employing symmetry property. In general, the proposed method is outperformed over than all available methods for pseudo Zernike moment's computations.

References

[1] Abdel-Qader H., Ramli A., and Al-Haddad S., "Fingerprint Recognition Using Zernike Moments," *The International Arab Journal of Information Technology*, vol. 4, no. 4, pp. 372-376, 2007.

[2] Al-Rawi M., "Fast Computation of Pseudo Zernike Moments," *Journal of Real-Time Image Processing*, vol. 5, no. 1, pp. 3-10, 2010.

[3] Bailey R. and Srinath M., "Orthogonal Moment Features for Use with Parametric and Non-Parametric Classifiers," *IEEE Transactions on Pattern Analysis and Machine Intelligence*, vol. 18, no. 4, pp. 389-399, 1996.

[4] Barchunova A. and Sommer G., "Recognition of Simple 3D Geometrical Objects Under Partial Occlusion," *in Proceedings of the 13th International Conference, Computer Analysis of Images and Patterns*, Berlin, Germany, vol. 5702, pp. 697-704, 2009.

[5] Bhatia A. and Wolf E., "On the Circle Polynomials of Zernike and Related Orthogonal Sets," *Proceedings of the Cambridge Philosophical Society*, vol. 50, no.1, pp. 40-48, 1954.

[6] Chergui L., Kef M., and Chikhi S., "Combining Neural Networks for Arabic Handwriting Recognition," *the International Arab Journal of Information Technology*, vol. 9, no. 6, pp. 588-595, 2012.

[7] Chong C., Raveendran P., and Mukundan R., "An Efficient Algorithm for Fast Computation of Pseudo-Zernike Moments," *the International Journal of Pattern Recognition and Artificial Intelligence*, vol. 17, no. 6, pp. 1011-1023, 2003.

[8] Haddadnia J., Ahmadi M., and Faez K., "An Efficient Feature Extraction Method with Pseudo-Zernike Moment in RBF Neural Network-Based Human Face Recognition System," *EURASIP Journal on Applied Signal Processing*, vol. 9, no. 2003, pp. 890-901, 2003.

[9] Haddadnia J., Ahmadi M., and Faez K., "An Efficient Method for Recognition of Human Faces Using Higher Orders Pseudo Zernike Moment Invariant," *in Proceedings of the 5th IEEE International Conference on Automatic Face and Gesture Recognition*, Washington, USA, pp. 330-335, 2002.

[10] Hosny K., "Exact and Fast Computation of Geometric Moments for Gray Level Images," *Applied Mathematics and Computation*, vol. 189, no. 2, pp. 1214-1222, 2007.

[11] Hosny K., "Fast and Accurate Method for Radial Moment's Computation," *Pattern Recognition Letters*, vol. 31, no. 2, pp. 143-150, 2010.

[12] Hosny K., "Fast Computation of Accurate Zernike Moments," *Journal of Real-Time Image Processing*, vol. 3, no. 1-2, pp. 97-107, 2008.

[13] Huang, R., Du M., and Liang G., "Spatially Weighted Pseudo-Zernike Moments for Human Face Recognition in Wavelet Domain," *Journal of Computational Information Systems*, vol. 5, no. 1, pp. 453-460, 2009.

[14] Ismail I., Shouman M., Hosny K., and AbdelSalam H., "Invariant Image Watermarking Using Accurate Zernike Moments," *Journal of Computer Science*, vol. 6, no. 1, pp. 52-59, 2010.

[15] Kanan H. and Faez K., "GA-Based Optimal Selection of PZMI Features for Face

Recognition," *Applied Mathematics and Computation*, vol. 205, no. 2, pp. 706-715, 2008.
[16] Kanan H., Faez K., and Gao Y., "Face Recognition Using Adaptively Weighted Patch PZM Array from a Single Exemplar Image Per Person," *Pattern Recognition*, vol. 41, no. 12, pp. 3799-3812, 2008.
[17] Leida L. and Baolong G., "Image Adaptive RST Invariant Watermark Using Pseudo-Zernike Moments," *Frontiers of Electrical and Electronic Engineering in China*, vol. 3, no. 1, pp. 20-24, 2008.
[18] Manjunath B., Salembier P., and Sikora T., *Introduction to MPEG-7: Multimedia Content Description Interface*, Wiley & Sons, USA, 2002.
[19] Mukundan R. and Ramakrishnan K., *Moment Functions in Image Analysis: Theory and Applications*, World Scientific, USA, 1998.
[20] Nabatchian A., Makaremi I., Abdel-Raheem E., and Ahmadi M., "Pseudo-Zernike Moment Invariants for Recognition of Faces Using Different Classifiers in FERET Database," *in Proceedings of the 3rd International Conference on Convergence and Hybrid Information Technology*, Busan, South Korea, pp. 933-936, 2008.
[21] Pang Y., Teoh B., and Ngo C., "Enhanced Pseudo Zernike Moments in Face Recognition," *IEICE Electronics Express*, vol. 2, no. 3, pp.70-75, 2005.
[22] Teague M., "Image Analysis via the General Theory of Moments," *Journal of Optical Society of America*, vol. 70, no. 8, pp. 920-930, 1980.
[23] Teh C. and Chin R., "On Image Analysis by the Method of Moments," *IEEE Transaction on Pattern Analysis and Machine Intelligence*, vol. 10, no. 4, pp. 496-513, 1988.
[24] Wang X., Hou L., and Yang H., "A Feature-Based Image Watermarking Scheme Robust to Local Geometrical Distortions," *Journal of Optics A: Pure and Applied Optics*, vol. 11, no. 6, 2009.
[25] Xin Y., Liao S., and Pawlak M., "Geometrically Robust Image Watermarking via Pseudo-Zernike Moments," *in Proceedings of the IEEE Candian Conference on Electrical and Computer Engineering*, vol. 2, pp. 939-942, 2004.
[26] Yang Z. and Guo B., "Image Registration Using Feature Points Extraction and Pseudo-Zernike Moments," *in Proceedings of the International Conference on Intelligent Information Hiding and Multimedia Signal Processing*, Harbin, China, pp. 752-755, 2008.

Khalid Hosny received his BSc, MSc and PhD from Zagazig University, Zagazig, Egypt in 1988, 1994, and 2000, respectively. From 1997 to 1999 he was a visiting scholar at: The University of Michigan, Ann Arbor and the University of Cincinnati, Cincinnati, USA. He joined the faculty of Computers and Informatics at Zagazig University, where he held the position of associate professor. He is a senior member of ACM, IEEE and the IEEE computer society. His research interests include image processing and pattern recognition. Dr. Hosny published more than 40 papers in international journals. He is a member of the editorial board and reviewer for many international journals in computer sciences and information technology.